

Encapsulation and Outdoor Testing of Perovskite Solar Cells: Comparing Industrially Relevant Process with a Simplified Lab Procedure

Quiterie Emery, Marko Remec, Gopinath Paramasivam, Stefan Janke, Janardan Dagar, Carolin Ulbrich, Rutger Schlatmann, Bernd Stannowski, Eva Unger, and Mark Khenkin*

Cite This: *ACS Appl. Mater. Interfaces* 2022, 14, 5159–5167

Read Online

ACCESS |

Metrics & More

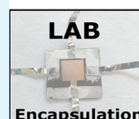

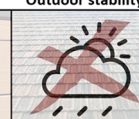



Article Recommendations

Supporting Information

ABSTRACT: Perovskite solar cells (PSCs) have shown great potential for next-generation photovoltaics. One of the main barriers to their commercial use is their poor long-term stability under ambient conditions and, in particular, their sensitivity to moisture and oxygen. Therefore, several encapsulation strategies are being developed in an attempt to improve the stability of PSCs in a humid environment. The lack of common testing procedures makes the comparison of encapsulation strategies challenging. In this paper, we optimized and investigated two common encapsulation strategies: lamination-based glass–glass encapsulation for outdoor operation and commercial use (COM) and a simple glue-based encapsulation mostly utilized for laboratory research purposes (LAB).

We compare both approaches and evaluate their effectiveness to impede humidity ingress under three different testing conditions: on-shelf storage at 21 °C and 30% relative humidity (RH) (ISOS-D1), damp heat exposure at 85 °C and 85% RH (ISOS-D3), and outdoor operational stability continuously monitoring device performance for 10 months under maximum power point tracking on a roof-top test site in Berlin, Germany (ISOS-O3). LAB encapsulation of perovskite devices consists of glue and a cover glass and can be performed at ambient temperature, in an inert environment without the need for complex equipment. This glue-based encapsulation procedure allowed PSCs to retain more than 93% of their conversion efficiency after 1566 h of storage in ambient atmosphere and, therefore, is sufficient and suitable as an interim encapsulation for cell transport or short-term experiments outside an inert atmosphere. However, this simple encapsulation does not pass the IEC 61215 damp heat test and hence results in a high probability of fast degradation of the cells under outdoor conditions. The COM encapsulation procedure requires the use of a vacuum laminator and the cells to be able to withstand a short period of air exposure and at least 20 min at elevated temperatures (in our case, 150 °C). This encapsulation method enabled the cells to pass the IEC 61215 damp heat test and even to retain over 95% of their initial efficiency after 1566 h in a damp heat chamber. Above all, passing the damp heat test for COM-encapsulated devices translates to devices fully retaining their initial efficiency for the full duration of the outdoor test (>10 months). To the best of the authors' knowledge, this is one of the longest outdoor stability demonstrations for PSCs published to date. We stress that both encapsulation approaches described in this work are useful for the scientific community as they fulfill different purposes: the COM for the realization of prototypes for long-term real-condition validation and, ultimately, commercialization of perovskite solar cells and the LAB procedure to enable testing and carrying out experiments on perovskite solar cells under noninert conditions.

KEYWORDS: perovskite solar cell, encapsulation, outdoor testing, IEC damp heat test, stability

	ISOS-D1 On-shelf stability	ISOS-O3 Outdoor stability	ISOS-D3 Damp heat stability
LAB Encapsulation			
COM Encapsulation			

1. INTRODUCTION

Over the past decade, tremendous progress has been made on improving the power conversion efficiency (PCE) of perovskite solar cells (PSCs), which has now reached 25.5%.¹ With low-cost and easily up-scalable fabrication methods, this photovoltaic (PV) technology is likely to play a key role in the future of solar energy.² PSCs suffer from both intrinsic and extrinsic instabilities, which need to be rectified for their further development and commercialization. The intrinsic instability of metal-halide perovskite absorber materials, found to be mostly due to dissociation of molecular cations and ion

migration, can be decreased by tuning the composition of the perovskite, transport layers, and electrodes.^{3,4} Chemical and physical changes in PSCs can be triggered by various environmental factors such as light, oxygen, temperature, and

Received: August 3, 2021

Accepted: December 7, 2021

Published: January 19, 2022



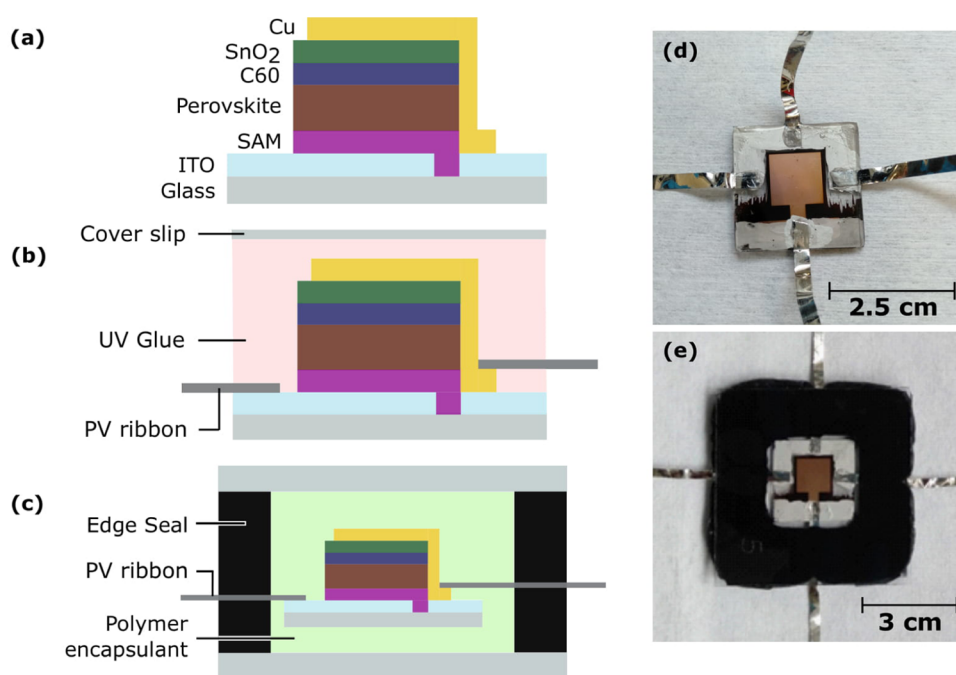


Figure 1. Cross-sectional views of (a) PSC stack, (b) glued (“LAB”), and (c) laminated (“COM”) samples. Photographs of (d) glued (“LAB”) and (e) laminated samples (“COM”) photographed from the back-contact side.

moisture.⁵ In particular, water is known to irreversibly catalyze the decomposition of the perovskite absorber.⁶ Several strategies, such as compositional engineering and surface passivation, have been developed to enhance the moisture stability of the devices.³ As for most thin-film photovoltaic devices, to prevent moisture and oxygen ingress into perovskite devices, and thus improve their extrinsic stability, specifically adapted encapsulation strategies are required compared to the standard procedures developed for crystalline silicon PV.

Requirements for materials chosen for the encapsulation of (perovskite) devices are: chemical inertness and no degradation of active devices layers upon deposition, resistance to ultraviolet (UV) radiation-induced degradation, >90% transmittance for the incident light, as well as a low water vapor transmission rate (WVTR) and oxygen transmission rate (OTR). A high electrical resistivity is also desirable to mitigate potential-induced degradation since it prevents leakage current which could degrade the cell. Mechanical properties such as flexibility, a high mechanical strength, adhesion to the contact surfaces within the module, and a thermal expansion coefficient matching that of PSC components are required to withstand long-term outdoor exposure in various climates.^{4,7} Moreover, the maximal thermal budget allowed to avoid damaging the cell during encapsulation depends on the materials used in the perovskite solar cell stack. Temperatures typically used for encapsulation of commercial c-Si PV modules exceed 150 °C,⁸ which might be too high for encapsulation of PSCs. Indeed, current standard perovskite-based devices often contain organic cations and organic contact layer materials exhibiting thermal degradation when heated to above 150 °C for extensive periods.

Glass–glass encapsulation, where the device is sandwiched between two glass sheets, is a common method reported for PSCs when flexible applications are not targeted.⁷ Note that encapsulation strategies for flexible PV application are beyond the scope of this paper. Recent achievements in this area are reported elsewhere.^{9–17} The symmetrical glass–glass config-

uration optimizes the mechanical stability of the packaging and reduces moisture penetration compared to the configuration with a polymer back-sheet, as it is often used for crystalline silicon PV modules.¹⁸ In PV modules using moisture-sensitive materials, such as various thin-film PV modules, an edge sealant, usually based on butyl rubber, is added. For laboratory test devices, several groups reported on using a UV curing epoxy glue as an edge sealant,^{19,20} sometimes in combination with Kapton tape over the active area²¹ or a piece of desiccant.^{22,23} However, due to their mechanical rigidity, epoxies are prone to cracking²⁴ and their curing process, which is exothermic, may damage the cell.²⁵ Other encapsulation strategies have been extensively reviewed and can be found elsewhere.^{4,5,7,25–27} Provided that the PSC stack is sufficiently thermally stable, the most promising route for its encapsulation implies the use of hot-melt polymer films, which avoids the usage of solvents.^{3,28} Such films typically need to be processed at a temperature between 100 and 150 °C to achieve their final stable properties, which can be detrimental to the PSC. Ethylene vinyl acetate (EVA), which is the most popular and cost-effective encapsulant for commercial silicon PV,²⁹ has also been used for the encapsulation of PSCs.^{30–32} Nonetheless, devices encapsulated with this polymer show a tendency to yellowing, browning, and delamination³³ and the acetic acid released during its aging can harm active layers in PSCs.²⁵ Therefore, alternatives to EVA, such as ionomers,^{21,34} polyurethane,³² or polyolefins (POE)^{32,35} have been investigated. Due to the lack of common standard testing conditions, it is not possible to compare results published for all of these different encapsulation materials.

Commercial PV modules presently offer a performance warranty period of >25 years, at the end of which their specified power output rating should not have decreased to less than typically 80% of the initial performance.³⁶ This is a very tough durability requirement for any emerging PV technology to match, especially if the technology would be combined with silicon to multijunction devices. Accelerated aging tests have

been developed by the International Electrotechnical Commission (IEC) to assess whether a PV technology has sufficient stability to meet these requirements. Among them, the IEC 61215 standard includes a damp heat (DH) test carried out for 1000 h at 85 °C and 85% relative humidity (RH), which is an accelerated test condition to evaluate the device resistance to high temperature and humidity on a long time scale.^{37,38} The ability of PSCs to pass the damp heat test was already demonstrated.^{35,39,40} To the best of our knowledge, there are no demonstrations that passing this crucial IEC test in fact results in the long operational stability under outdoor conditions; therefore, further verification is required.

In addition to the need to develop strategies that enable PSCs to demonstrate long-term stability requirements making this technology suitable/feasible for the PV market, encapsulation is also often required as a short-term measure in research laboratories for, e.g., sample storage, transport, or characterization outside the inert environment of gloveboxes. Complex lamination equipment, however, is rarely available in research groups and needs space and investment to be integrated inside glovebox environments where devices are most often manufactured. Thus, it is of high value for the research to develop and utilize encapsulation procedures that can be realized with small footprint and negligible investment cost inside gloveboxes.

In this work, we therefore compare two different complementary encapsulation approaches for PSCs: a glue-based encapsulation method that can be easily implemented manually enabling simple encapsulation of samples even inside gloveboxes, which we refer to as the LAB method, and a lamination-based encapsulation procedure enabling prototype manufacturing for pre-commercialization validation, here referred to as the COM method.

We compared the effectiveness of these two encapsulation strategies for PSCs by carrying out on-shelf storage, damp heat testing, and outdoor operation.

2. RESULTS AND DISCUSSION

2.1. Encapsulation Techniques. To be able to accurately compare the two aforementioned encapsulation styles, the same solar cell stack was used for both. To prevent temperature degradation from lamination, a formamidinium/cesium (FACs)-based perovskite absorber was chosen as the absorber, which exhibits signs of degradation first at temperatures >150 °C.⁴¹ The other layers and fabrication of the p–i–n cell stack used in this study are described in the [Experimental Section](#) and represented in [Figure 1a](#).

2.1.1. Glue-Based “LAB” Encapsulation. For the glue-based encapsulation technique, which we will refer to below as LAB encapsulation, a thin glass coverslip was glued on top of the cell with a UV light curing acrylate adhesive ([Figure 1b,d](#)). In the [Supporting Information](#), the optimization of this encapsulation method comparing different UV glues, UV curing durations, and cover glass geometries (cavity glass with glue applied on the edges only or flat coverslip with glue applied all over the active area) are described ([Figures S1 and S2](#)). As one of the results of these preliminary investigations, we found that when the size of the cover glass was smaller than the substrate area of the lab test devices and did not fully cover the metal contacts to the top and bottom electrodes, rapid degradation upon exposure to humidity was observed ([Figure S3](#)), as also previously reported by Weerasinghe et al.¹² Therefore, glass coverslips of 24 × 24 mm² almost matching the substrate size were utilized for the LAB-type encapsulation in this work. To make contact with the

solar cell pixels of the test device, tinned copper ribbons (PV ribbons) were glued to the top and bottom electrodes enabling to cover the whole device with glue as illustrated in [Figure 1b,d](#). Extra care should be taken during encapsulation to minimize the pressure applied on the coverslip during the UV curing of the glue. Indeed, we suspect that applying too much force on the substrate can directly damage the perovskite underneath ([Figure S4](#)). After encapsulation, a slight drop in the short-circuit current density (J_{sc}) of the cells was observed ([Figure S5](#)). We speculate that this is due to a too long air exposure of the cells before their encapsulation because most of the time, the J_{sc} value of the cells was not affected by encapsulation in our preliminary study ([Figures S1 and S2](#)).

2.1.2. Lamination-Based “COM” Encapsulation. The second encapsulation technique that we will herein refer to as COM encapsulation consists of a butyl rubber edge sealant and a polyolefin (POE) film as an encapsulant ([Figure 1c,e](#)), as often used for commercial thin-film modules such as CIGS. This set of materials has already been reported as promising to enable the commercial viability of PSCs.³⁵ The butyl rubber edge sealant with added desiccant is the main component to prevent moisture and oxygen ingress into the device.⁴² Indeed, it is chosen for its low WVTR, a parameter used to measure the barrier properties of a material rather than OTR since water vapor molecules are smaller than oxygen molecules and, therefore, harder to be blocked.²⁵ The butyl rubber edge sealant also has a low glass-transition temperature (below –50 °C),³⁵ which is compliant with mechanical stress implied by extreme weather conditions.²⁴ It is supplied in the form of a tape and therefore very convenient to apply. The polyolefin used presents a low Young's modulus (8 MPa), which contributes to the mechanical stability of the packaging,³⁴ and a high volumetric resistivity ($\geq 10^{17}$ Ω cm at 23 °C) so that potential-induced degradation is less likely to occur.²⁵ This encapsulation type is carried out inside a vacuum laminator, which enables to avoid air trapping inside the package and to evenly melt and cure the POE foil and the edge seal. The final thickness of the package needs to be as homogeneous as possible to allow it to retain its mechanical stability. In contrast to what is usually done for commercial thin-film modules, we encapsulated the cell stack, including the thin glass superstrate, between two glass sheets. This was done to allow for enough space for edge sealing (at least 10 mm) around the active cell area, but can be avoided in the future by processing PSCs on larger glasses. We speculate that this does not affect the DH or outdoor stability of the device. However, additional reflection and parasitic absorption losses reduce the photocurrent ([Figure S5](#)). In optimized devices and modules for commercial applications, the device and encapsulation geometry need to be further optimized to minimize optical and electrical losses.

2.2. On-Shelf and Damp Heat Stability Testing. Encapsulated solar cells of each encapsulation technique, i.e., LAB and COM, were divided into three subsets which were respectively submitted to different storage conditions. We here employed “on-shelf” storage in the dark at 21 ± 2 °C, $30 \pm 3\%$ relative humidity (RH). The second test condition was exposing samples to 85 °C and 85% RH damp heat (DH) test according to the IEC 61215 standard. The third test condition was an outdoor operation in a roof-top test installation in Berlin, Germany (November 2020 to September 2021). These experiments correspond to ISOS-D1, ISOS-D3, and ISOS-O3 research protocols for solar cell aging, respectively.^{43,44} A

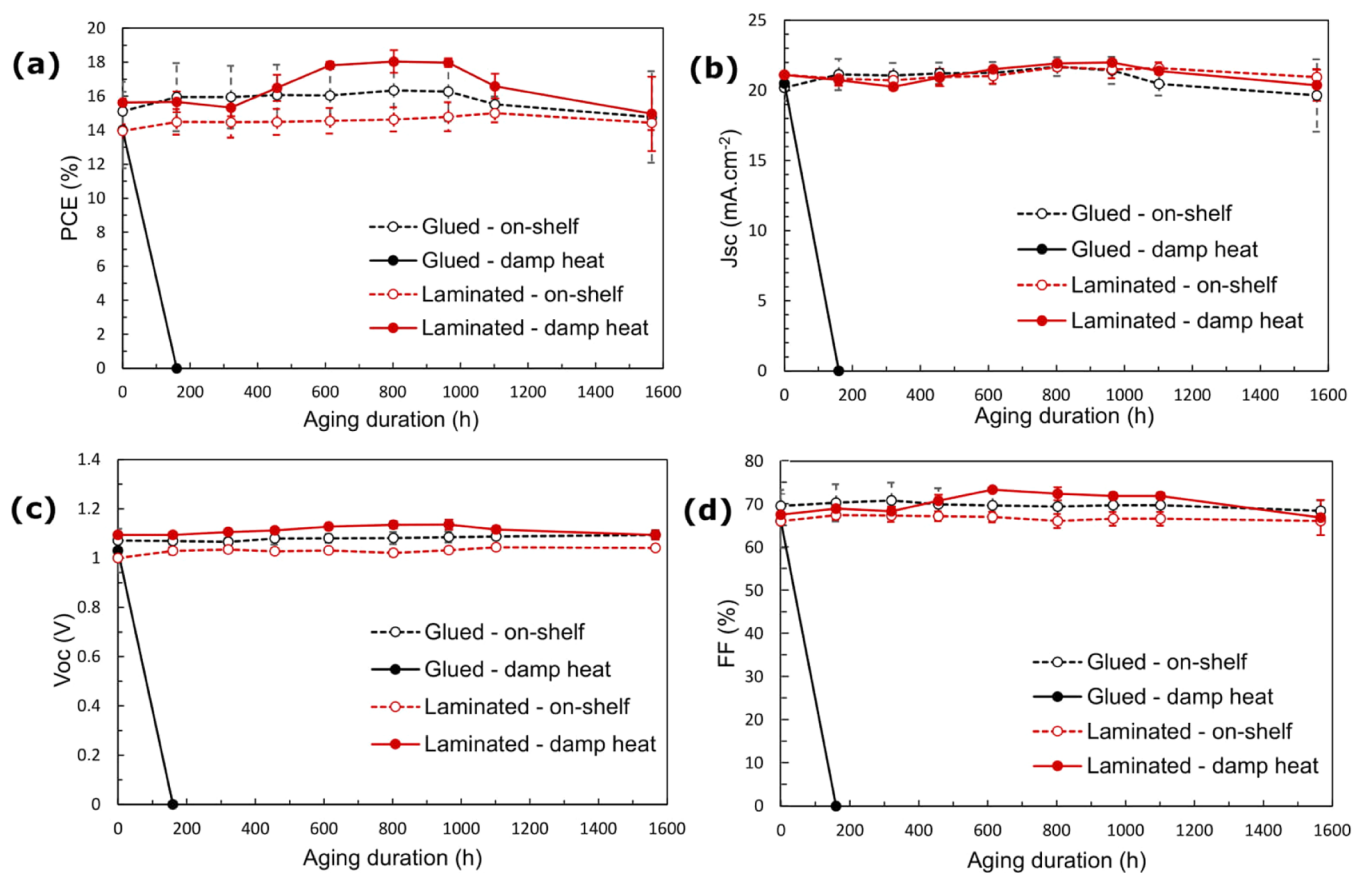


Figure 2. Evolution of the average (a) PCE, (b) J_{sc} , (c) V_{oc} , and (d) fill factor (FF) (over two to three samples) with standard deviation of glued (“LAB”) and laminated (“COM”) cells with on-shelf (in the dark, 21 °C, 30% RH, ISOS-D1) or damp heat (85 °C, 85% RH, ISOS-D3) storage under indoor standard testing conditions. The evolution of the normalized efficiency is shown in Figure S6.

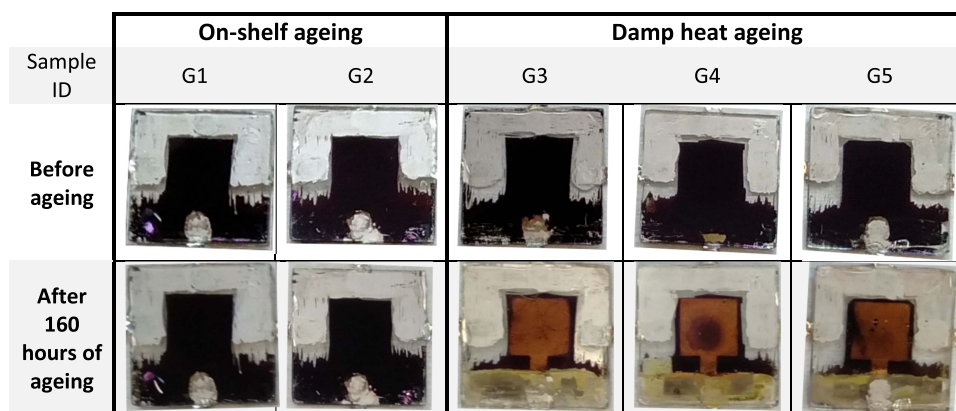


Figure 3. Photographs from the glass substrate side of glue-encapsulated (“LAB”) cells before and after 160 h of on-shelf ageing (in the dark, 21 °C, 30% RH) or 160 h of damp heat exposure (85 °C, 85% RH). After DH exposure, the back-electrode is visible due to severe absorber layer degradation.

descriptive table of the cells used in this study is provided in Table S1.

Figure 2 shows the evolution of the I - V parameters of cells with on-shelf and damp heat aging over 1566 h. LAB encapsulation allows cell to retain more than 93% of their efficiency after 1566 h on-shelf (see Figure S6 for the normalized efficiency). Therefore, we speculate that this encapsulation would be suitable for sample exchange or characterization outside of the glovebox where the RH is usually between 30 and 50%. Already after the first step in time in the DH experiment (160 h of aging in the chamber), the perovskite of each of the

three LAB test-cells had changed color from dark brown to yellow (Figure 3), which is likely due to perovskite decomposition⁴⁵ and their efficiency dropped to zero (Figure 2). An additional DH experiment that resolves with much smaller time steps the degradation of COM cells is shown in Figure S7. The experiment shows that after 8 h of damp heat exposure, LAB cells retain over 98% of their initial efficiency but it has quickly dropped to 45 and 32% after 24 and 48 h, respectively. Furthermore, after 24 h, edges of the cells switch from a dark color to yellow (Figure S8). This degradation also translates into a homogeneous drop in the external quantum

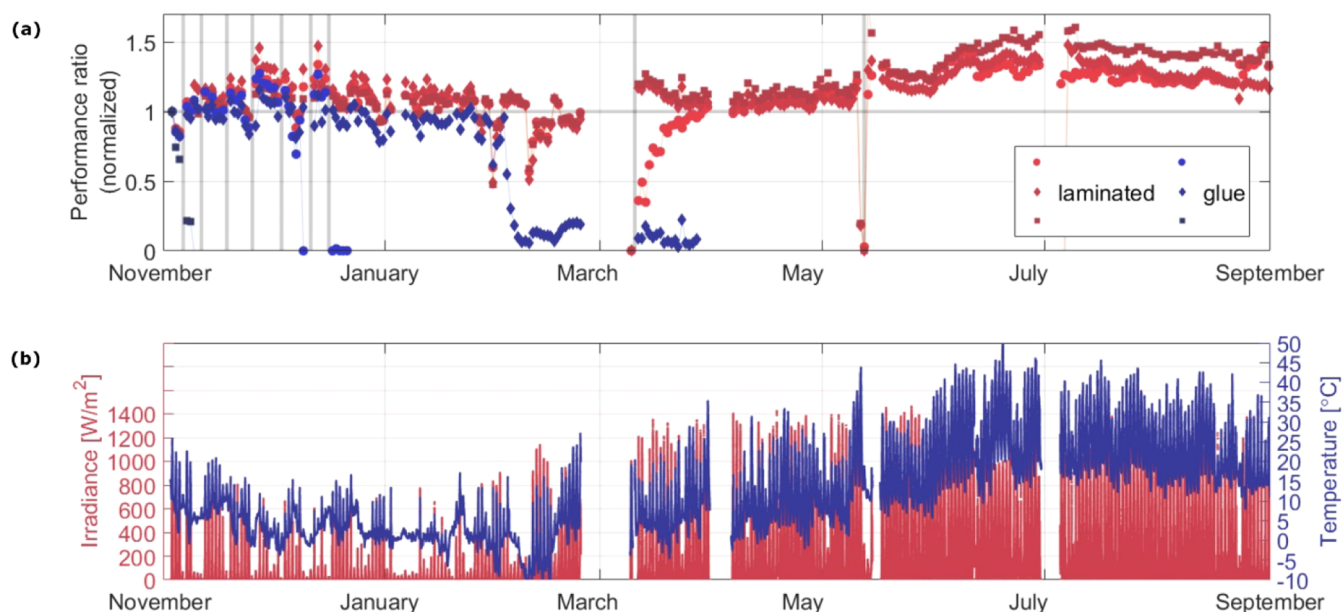


Figure 4. (a) Evolution of PSC performance ratio of glued (“LAB”) and laminated (“COM”) cells during the outdoor exposure. Days of indoor control measurements are shown in gray. (b) Irradiance in the plane of cells and cell temperature during the outdoor experiment.

efficiency (EQE) signal over the entire measured wavelength range (Figure S9). Laminated COM cells, on the contrary, passed the DH test and their efficiency was even improved after 1000 h in DH treatment. After 1566 h, the cells retained on average more than 95% of their initial efficiency.

The performance of glued and laminated cells, which were stored on-shelf, slightly improved in the first 1000 h and, in particular, in the first 200 h. Several explanations have been hypothesized in the literature to explain this initial enhancement. It could be attributed to the release of residual stress and lattice distortion,⁴⁶ the coalescence of small crystallites into larger ones in the perovskite thin-film,^{46,47} or the passivation of perovskite by sodium-ion diffusion from the indium tin oxide (ITO) glass substrate.⁴⁸

Interestingly, it appears that this performance enhancement is even more pronounced for cells that were exposed to DH, between 450 and 960 h, possibly due to the elevated temperatures (Figure S10). It seems that damp heat treatment results in two opposite phenomena on laminated cells, which are respectively beneficial and detrimental to the cells. To determine if damp heat treatment modified the composition of the perovskite, and therefore its band gap, external quantum efficiency (EQE) measurements were taken on laminated cells after 1140 h of damp heat or on-shelf aging (Figure S11). The EQE response of laminated cells exposed to 85 °C, 85% RH is similar to the one of those aged in 21 °C at 30% RH in the long-wavelength region, which shows that at this stage of the experiment, the optical band gap and spectral response of these cells were similar. This is consistent with a fairly constant short-circuit current (J_{sc}) throughout the experiment. Instead, the fill factor (FF) is the main parameter that differs between laminated (COM) cells exposed to damp heat and cells stored on-shelf. We hypothesize that exposing samples to damp heat might initially lead to a slight degradation of $\text{Cs}_{0.15}\text{FA}_{0.85}\text{PbI}_{2.55}\text{Br}_{0.45}$ to form some PbI_2 , acting as a passivation center, as it has been reported for short-time exposure of triple cation perovskite thin films to 85 °C.⁴⁹ Follow-up studies to this work are needed to investigate specific changes in the absorber layer composition and microstructure as well as interfacial properties within the device

stack to explain the intermittent performance enhancement upon DH test condition exposure.

2.3. Outdoor Stability Testing. To examine the durability of both encapsulation types under outdoor operational conditions, six devices were exposed and tested in an outdoor testing setup in Berlin, Germany. In the period of November 2020 to September 2021, the cells were placed on an open rack (tilted 35° facing south) and connected to a maximum power point (MPP) tracking system. Periodically, the cells were disconnected for indoor J - V and electroluminescence (EL) measurements. Fall and winter months in Berlin are not particularly sunny but have a lot of precipitation and RH between 60 and 100%. Thus, the conditions present a significant challenge for the role of encapsulation.

Figure 4 shows 10 months of outdoor exposure for the PSCs of both encapsulation approaches. Device power output and PCE at a particular point of time depend on weather conditions (mostly irradiance and temperature, Figure 4b) and the accumulated light soaking (see Figure S15 for two examples of diurnal variations on sunny and cloudy days). Typically in the morning, we observe an improvement in the conversion efficiency over several hours due to the light soaking effect, which is especially noticeable on cloudy days. The particular shape of diurnal dependence varies from day to day (Figure S16a). As a metric to quantify the device stability, we use the performance ratio (PR) for each day. The PR is the ratio between measured and expected power output of the device (see the Experimental Section and Figure S17 for details and the applied filtering procedure for very dark days).

As immediately visible in Figure 4, one sample with LAB encapsulation retained its initial performance for 3 months of continuous testing outdoors. While outdoor measurements under MPP tracking show a sharp drop in its performance during the fourth month outdoor, indoor control measurements (Figure S12) show that the cell retained 78% of its initial efficiency after 4 months and 49% after 6 months outdoors. We think that this difference between outdoor and indoor measurements could be explained by a contacting issue during the fourth month of outdoor MPP tracking of the cell. The two

Table 1. Summary of the Characteristics of Each Encapsulation Technique

	LAB encapsulation	COM encapsulation
material required	UV-curable adhesive, coverslip, contacting ribbons, conductive glue, and UV lamp	encapsulant film, edge sealant, encapsulation glasses, contacting ribbons, conductive glue, and vacuum laminator
temperature of the process	ambient (UV curing)	150 °C for 20 min
suitable for air-sensitive materials	yes, process can be carried out in a glovebox.	no, samples have to be exposed to air during transfer into the laminator
outcome of stability tests: ISOS-D1	good on-shelf stability (>1500 h, no losses)	good on-shelf stability (>1500 h, no losses)
ISOS-O3	inconsistent outdoor stability (days–months to fully degrade)	good outdoor stability (>6 months, no losses)
ISOS-D3	fails damp heat test (PCE more than halved after 24 h)	passed damp heat test (>1500 h, >90% PCE)
recommendation	suitable for samples shipping and short-term test on samples outside gloveboxes	suitable encapsulation strategy even for prototype validation; optical losses need to be minimized

other LAB-encapsulated cells, however, failed after 6 weeks and only 4 days, respectively. The very fast failure of the latter is likely due to mechanical stress created by an uneven encapsulation processing (Figure S4). We believe that such a huge difference in the outdoor lifetimes of LAB samples is due to the manual application of the glue, experience, and a large degree of automation of the encapsulation step that will help to produce more consistent encapsulations. Even though we considered the LAB encapsulation strategy to be merely a short-term measure to enable experiments outside a glovebox environment, this encapsulation has prospects of enabling at least several weeks of outdoor lifetime. EL images, which were also periodically taken on encapsulated samples, allow for spatially resolved performance analysis (Figure S13). The uniformity of EL images of LAB-encapsulated samples changed more dramatically over time than the uniformity of images of COM-encapsulated samples. Darker regions, likely due to increased local series resistance,⁵⁰ evolve randomly around local defects of the cells and also seem to appear and progress from the edge of the device, which we think could be due to humidity ingress.

In contrast, COM encapsulation, which had also passed the DH test, shows excellent stability barely losing performance after 10 months outdoors. This observation is supported by control J – V measurements under the sun simulator (Figure S12). Moreover, the uniformity of EL images of COM-encapsulated samples is relatively constant over the duration of outdoor exposure.

Table 1 highlights the complementarity between the two encapsulation approaches compared in this study. The LAB encapsulation can provide on-shelf stability to materials that are vulnerable to air or heat, without requiring complex equipment, while the COM encapsulation appears to be very promising for industrial applications where long-term stability of the cells is required in outdoor environment.

Similar to the indoor aging (Figure 2), PSCs investigated in this study show a pronounced improvement in the beginning of the outdoor exposure. Indoor control measurements show a gradual increase in the V_{oc} , which is responsible for this performance gain (Figure S12). The origin of this improvement is likely to be the same in all experiments; however, in fall-winter, in Berlin, it takes about 1 month to saturate the effect. After the

improvement is saturated, the PR of laminated PSCs slowly declines.

Gray lines in Figure 4a represent single days when devices were taken down for indoor measurements. They mostly spent time in the dark during those days. Almost every time after such a day, we observed significant improvement in the PR. Note that the encapsulation glasses were cleaned before each indoor measurement, which could explain this improvement. However, we believe that the reason is a different one, see Figure S16b,c, i.e., the improvement is due to the recovery effects previously reported in PSCs.⁵¹ Certainly, the recovery present in the normal operation of the device during every night is only more pronounced after measurement days due to a longer period of recovery. It is likely that night-time recovery contributes to the encouraging long measured outdoor lifetimes in this work.

3. CONCLUSIONS

We presented two complementary encapsulation strategies for perovskite solar devices. One of them, a glue-based encapsulation (LAB), provides satisfying protection of PSCs against ambient conditions and can be employed using very simple equipment. This encapsulation is therefore particularly suitable for air- or temperature-sensitive devices as the process can be carried out at room temperature and inside a glovebox. Simple “glue-based” encapsulation methods are enabling short-term sample protection for, e.g., shipment or some tests outside glovebox atmospheres. We here show that such encapsulation can last up to 3 months and can probably even be improved using other types of glues. However, for long-term device operation, this encapsulation is likely less suitable as our damp heat tests demonstrate: barriers and mechanical properties of the glues are not sufficient to sustain harsh testing conditions. The lamination-based COM encapsulation method investigated here, using POE + butyl lamination in a glass–glass stack, is more difficult to implement technically but provides excellent stability even under damp heat and outdoor test conditions. Lamination restricts the type of devices that can be encapsulated as it requires samples to be exposed to ambient air for a short period of time and, even more demanding, heating samples to 150 °C for 20 min for the lamination process. However, it was found to provide excellent long-term stability in DH and outdoor testing, a prerequisite for the commercialization of

PSCs. In particular, the COM encapsulation method enabled devices to fully retain their initial efficiency after more than 10 months of outdoor exposure in Berlin, which is one of the longest stable outdoor efficiency values for PSCs published to date.

4. EXPERIMENTAL SECTION

4.1. Materials for Solar Cell Fabrication. Lead(II) iodide (PbI_2 , 99.99%, trace metals basis), lead(II) bromide (PbBr_2 , purity >98.0%), and 2PACz (purity >98.0%) were purchased from Tokyo Chemical Industry (TCI). Anhydrous ethanol was achieved from VWR Chemicals. Cesium iodide (CsI , 99.999% Cs) and formamidinium iodide (FAI, 99.99%, trace metals basis) were obtained from abcr GmbH and Dyenamo, respectively. Dimethyl sulfoxide (DMSO), dimethylformamide (DMF), and anisole were purchased from Sigma-Aldrich. C_{60} (sublimed) was bought from CreaPhys GmbH. All of the chemicals were used as it is without any further purification.

4.2. Perovskite Precursor Inks Preparation. A perovskite "FACs" ($\text{Cs}_{0.15}\text{FA}_{0.85}\text{PbI}_{2.55}\text{Br}_{0.45}$) precursor solution of 1.3 M concentration was prepared by dissolving PbI_2 (464.5 mg), PbBr_2 (107.4 mg), FAI (190.0 mg), and CsI (50.6 mg) powders in DMF/DMSO (4:1) in a single vial. The solution was kept on a shaker at 60 °C until it appeared transparent. The final FACs ink was filtered using a 0.2 μm sized poly(tetrafluoroethylene) (PTFE) filter before spin-coating.

4.3. Solar Cell Fabrication. Perovskite solar cells with p-i-n structure with layer configuration of ITO|2PACz| $\text{Cs}_{0.15}\text{FA}_{0.85}\text{PbI}_{2.55}\text{Br}_{0.45}$ | C_{60} | SnO_2 |Cu were fabricated on a pre-patterned tin-doped indium oxide (ITO) glass substrate of 25 × 25 mm², with a sheet resistance of 15 Ω (Automatic Research GmbH). The patterned ITO substrates were cleaned sequentially in Mucosal soap solution, deionized (DI), water, acetone, and isopropanol via ultrasonication for 15 min of each and followed by UV-ozone treatment (UVOH150 LAB from FHR) for 15 min. Next, all substrates were transferred in a N_2 -filled glovebox (MBraun) where 1 mmol/L 2PACz solution was spin-coated on cleaned ITO substrate at the speed of 3000 rpm for 30 s. The substrates were annealed at a temperature of 100 °C for 10 min. The perovskite solution was spin-coated on ITO + self-assembled monolayer (SAM) substrates with a speed of 3500 rpm with 5 s acceleration for 40 s (MBraun MB SC-210). Anisole (250 μL) was dropped on the wet perovskite after 30 s. The films were then annealed at 100 °C for 30 min on a hot plate. Afterward, the substrates were transferred into an evaporation chamber (MBraun ProVap 3G) where 23 nm of C_{60} was thermally evaporated on the perovskite layer at a rate of 0.04–0.10 $\text{\AA}/\text{s}$ at a base pressure of 1×10^{-6} mbar. Next, a 20 nm of SnO_2 layer was deposited using atomic layer deposition (ALD) in an Arradiance GEMStar reactor according to the same procedure as described previously.⁵² Finally, 100 nm of Cu was deposited by thermal evaporation at a rate of 0.03–1.2 $\text{\AA}/\text{s}$ at a base pressure of 1×10^{-6} mbar (MBraun ProVap 3G).

4.4. Solar Cell Encapsulation. To access the contacts of the cells after encapsulation, tinned copper solar ribbons (Ulbrich, part#7746-9062) were glued with a polyurethane conductive adhesive (Polytec PU1000) to the cathodes and anodes on the 25 × 25 × 1.1 mm³ substrates. The glue was cured at 100 °C for 10 min.

4.4.1. Glue ("LAB") Encapsulation. Inside a nitrogen-filled glovebox, a UV-light curing adhesive (Polytec UV2137 DC) was deposited all over the surface of the substrate and a 24 × 24 mm² flat coverslip was laid on top. The glue was cured by gently pressing over the coverslip and applying about 15 s of UV irradiation (395 nm).

4.4.2. Lamination ("COM"). Each substrate was sandwiched between two pieces of 60 mm × 60 mm × 2.1 mm glass (Planiclear, Saint-Gobain) with two 25 mm × 25 mm pieces of polyolefin encapsulant (Mitsui, Solar ASCE TR02BA, 500 μm) between the substrate and the top glass and two pieces of encapsulant between the substrate and the bottom glass. A butyl rubber edge seal with added desiccant (Quanex SET LP03, 3948) was applied as a frame on the glass, 0.5 cm from its edges. The solar ribbons were laid between the top and bottom butyl edge seal, which were, respectively, 1.2 and 2.4 mm thick. The package was laminated in a vacuum laminator (Meier Solar

Solution, ICOLAM 10/08) at 150 °C. The vacuum of the chamber was pulled down to the minimum during 4 min. Then, the pressure applied on the package was gradually increased for 2 min up to 900 mbar and maintained at 900 mbar for 14 min before the pressure was released and the chamber was brought back to atmospheric pressure. The samples were finally allowed to air cool outside the laminator.

4.5. Photovoltaic Characterization. Cells with an active area of 1 cm² were measured without shadow masks. Current–voltage (J – V) measurements were performed under AM1.5G (1 sun) equivalent illumination with a calibrated Wavelabs Sinus-70 LED class AAA sun simulator. A Keithley 2400 source-measure unit and a LabView control program were used. Samples were placed on a cooling stage at a temperature of 25 °C. The light intensity was calibrated with a KG3 silicon reference solar cell. The voltage was scanned in both directions between 1.25 and –0.2 V with a step size of 0.02 V, an integration time of 20 ms, and a settling time of 40 ms. The value of each parameter (PCE, FF, V_{oc} , and J_{sc}) retained for each data point was the one related to the best PCE obtained over 40–60 consecutive J – V measurements, which corresponds to about 30 min of light soaking. The J_{sc} value of the cells typically decreased with light soaking (and thus, consecutive measurements), while V_{oc} and FF increased. This generally led to an increase in the PCE of the cells during the first J – V measurements until it started to decrease. After encapsulation, the average variation between the PCE measured in forward and reverse scan directions was 5.2%. A representative J – V curve of fresh encapsulated cells is shown in Figure S18. EQE measurements were obtained with a home-built setup using chopped (78 Hz) monochromatic light from a xenon lamp and a halogen lamp and equipped with a source meter (Agilent 34401A) and a digital lock-in amplifier (SRS 810).

4.6. Stability Testing. **4.6.1. On-Shelf Stability and Damp Heat Testing.** Glued and laminated cells were aged in a cabinet with a monitored temperature of 21 ± 2 °C and relative humidity of $30 \pm 3\%$ for on-shelf stability testing and in an environmental chamber (Weiss WK11-600/40) at 85 °C, 85% RH for damp heat stability testing. Samples were periodically taken out of the chamber and cabinet for I – V and EL measurements. Samples coming out of the damp heat chamber were cooled in air for 1 h prior to any measurement.

4.6.2. Outdoor Testing. Outdoor exposure experiments were carried out on the roof-top setup located in Berlin, Germany ($52^\circ 25' 53.5''\text{N}$, $13^\circ 31' 27.7''\text{E}$). Encapsulated PSCs were fixed on a 35° tilted stand facing south. Each cell was connected to maximum power point tracking system (MP2005M6, LPVO), which utilizes a perturb and observe algorithm. Irradiance in the plane of solar cells was measured every 2 s with an EKO ML-02 Si-pyranometer. The cell temperature was measured with the DS18B20 temperature sensors attached to the rear side of the encapsulated cells. Ambient temperature, relative humidity, and precipitation were measured with a meteo station (CLIMA SENSOR US 4.920x.00.00x) located at the test field.

To trace device degradation, we used performance ratio (PR), calculated as

$$\text{PR} = \frac{\int_{00:00}^{23:59} P_{\text{MPP}}(t) dt}{\text{PCE} \times \int_{00:00}^{23:59} P_{\text{in}}(t) dt}$$

where PCE is the initial cell efficiency, measured under sun simulator. In the calculation of PR, only days with insolation P_{in} greater than 0.17 kWh/m² were included (see Figure S17).

4.7. EL Measurements. EL images on encapsulated samples exposed outdoor were periodically taken after J – V measurements with a LumiSolarMobile System from GreatEyes. The maximal current was set to 50 mA, and the maximal voltage to 1.5 V. Unless specified otherwise, consistent integration times (between 300 and 500 ms) throughout outdoor exposure duration were chosen for each sample and 10 s of current soaking was applied prior to each measurement.

■ ASSOCIATED CONTENT

Supporting Information

The Supporting Information is available free of charge at <https://pubs.acs.org/doi/10.1021/acsami.1c14720>.

Additional experimental details and results, further sample characterization, descriptive table of the cells mentioned in this article, EQE spectra, and EL images (PDF)

AUTHOR INFORMATION

Corresponding Author

Mark Khenkin – Helmholtz-Zentrum Berlin für Materialien und Energie GmbH, 12489 Berlin, Germany; orcid.org/0000-0001-9201-0238; Email: mark.khenkin@helmholtz-berlin.de

Authors

Quiterie Emery – Helmholtz-Zentrum Berlin für Materialien und Energie GmbH, 12489 Berlin, Germany; orcid.org/0000-0003-1422-9677

Marko Remec – Helmholtz-Zentrum Berlin für Materialien und Energie GmbH, 12489 Berlin, Germany; Faculty of Electrical Engineering, University of Ljubljana, 1000 Ljubljana, Slovenia

Gopinath Paramasivam – Helmholtz-Zentrum Berlin für Materialien und Energie GmbH, 12489 Berlin, Germany

Stefan Janke – Helmholtz-Zentrum Berlin für Materialien und Energie GmbH, 12489 Berlin, Germany

Janardan Dagar – Helmholtz-Zentrum Berlin für Materialien und Energie GmbH, 12489 Berlin, Germany

Carolyn Ulbrich – Helmholtz-Zentrum Berlin für Materialien und Energie GmbH, 12489 Berlin, Germany

Rutger Schlatmann – Helmholtz-Zentrum Berlin für Materialien und Energie GmbH, 12489 Berlin, Germany; orcid.org/0000-0002-5951-9435

Bernd Stannowski – Helmholtz-Zentrum Berlin für Materialien und Energie GmbH, 12489 Berlin, Germany

Eva Unger – Helmholtz-Zentrum Berlin für Materialien und Energie GmbH, 12489 Berlin, Germany; orcid.org/0000-0002-3343-867X

Complete contact information is available at: <https://pubs.acs.org/10.1021/acsami.1c14720>

Notes

The authors declare no competing financial interest.

ACKNOWLEDGMENTS

Q.E., G.P., J.D., and E.U. acknowledge funding from the BMBF-funded project SNaPSHoTs (grant no. 01I01806). M.R. and M.K. acknowledge the support of European partnering protect TAPAS (PIE-0015). C.U. and R.S. acknowledge support by the Helmholtz Association under the program “Energy System Design”. M.R. and G.P. are members of the HyPerCells graduate school. G.P. is a member of the HI-SCORE research school at HZB. All authors thank Ulas Erdil for providing additional samples for the damp heat experiment.

REFERENCES

- (1) NREL. <https://www.nrel.gov/pv/assets/pdfs/best-research-cell-efficiencies-rev210726.pdf> (accessed Sept 24, 2021).
- (2) Yang, Z.; Babu, B. H.; Wu, S.; Liu, T.; Fang, S.; Xiong, Z.; Han, L.; Chen, W. Review on Practical Interface Engineering of Perovskite Solar Cells: From Efficiency to Stability. *Sol. RRL* **2020**, *4*, No. 1900257.
- (3) Zhang, S.; Han, G. Intrinsic and Environmental Stability Issues of Perovskite Photovoltaics. *Prog. Energy* **2020**, *2*, No. 022002.
- (4) Uddin, A.; Upama, M.; Yi, H.; Duan, L. Encapsulation of Organic and Perovskite Solar Cells: A Review. *Coatings* **2019**, *9*, No. 65.
- (5) Li, D.; Zhang, D.; Lim, K.-S.; Hu, Y.; Rong, Y.; Mei, A.; Park, N.-G.; Han, H. A Review on Scaling Up Perovskite Solar Cells. *Adv. Funct. Mater.* **2020**, *31*, No. 2008621.
- (6) Wang, D.; Wright, M.; Elumalai, N. K.; Uddin, A. Stability of Perovskite Solar Cells. *Sol. Energy Mater. Sol. Cells* **2016**, *147*, 255–275.
- (7) Corsini, F.; Griffini, G. Recent Progress in Encapsulation Strategies to Enhance the Stability of Organometal Halide Perovskite Solar Cells. *J. Phys.: Energy* **2020**, *2*, No. 031002.
- (8) Wiesmeier, C.; Haedrich, I.; Weiss, K.-A.; Duerr, I. Overview of PV Module Encapsulation Materials. *Photovoltaics Int.* **2013**, *19*, 85–92.
- (9) Mohammadi, M.; Gholipour, S.; Malekshahi Byranvand, M.; Abdi, Y.; Taghavinia, N.; Saliba, M. Encapsulation Strategies for Highly Stable Perovskite Solar Cells under Severe Stress Testing: Damp Heat, Freezing, and Outdoor Illumination Conditions. *ACS Appl. Mater. Interfaces* **2021**, *13*, 45455–45464.
- (10) Kim, J.; Jang, J. H.; Kim, J.-H.; Park, K.; Jang, J. S.; Park, J.; Park, N. Inorganic Encapsulation Method Using Solution-Processible Polysilazane for Flexible Solar Cells. *ACS Appl. Energy Mater.* **2020**, *3*, 9257–9263.
- (11) Han, G. S.; Yoo, J. S.; Yu, F.; Duff, M. L.; Kang, B. K.; Lee, J.-K. Highly Stable Perovskite Solar Cells in Humid and Hot Environment. *J. Mater. Chem. A* **2017**, *5*, 14733–14740.
- (12) Weerasinghe, H. C.; Dkhissi, Y.; Scully, A. D.; Caruso, R. A.; Cheng, Y. B. Encapsulation for Improving the Lifetime of Flexible Perovskite Solar Cells. *Nano Energy* **2015**, *18*, 118–125.
- (13) Li, B.; Wang, M.; Subair, R.; Cao, G.; Tian, J. Significant Stability Enhancement of Perovskite Solar Cells by Facile Adhesive Encapsulation. *J. Phys. Chem. C* **2018**, *122*, 25260–25267.
- (14) Rolston, N.; Printz, A. D.; Hilt, F.; Hovish, M. Q.; Brüning, K.; Tassone, C. J.; Dauskardt, R. H. Improved Stability and Efficiency of Perovskite Solar Cells with Submicron Flexible Barrier Films Deposited in Air. *J. Mater. Chem. A* **2017**, *5*, 22975–22983.
- (15) Zhao, O.; Ding, Y.; Pan, Z.; Rolston, N.; Zhang, J.; Dauskardt, R. H. Open-Air Plasma-Deposited Multilayer Thin-Film Moisture Barriers. *ACS Appl. Mater. Interfaces* **2020**, *12*, 26405–26412.
- (16) Zhu, L.; Babu, S. S.; Yu, Q.; Long, Y.; Zheng, Z.; Wu, H.; Liu, S.; Chi, Z.; Zhang, Y.; Xu, J. Transparent Flexible Ultra-Low Permeability Encapsulation Film: Fusible Glass Fired on Heat-Resistant Polyimide Membrane. *Adv. Mater. Interfaces* **2020**, *7*, No. 2001170.
- (17) Sutherland, L. J.; Weerasinghe, H. C.; Simon, G. P. A Review on Emerging Barrier Materials and Encapsulation Strategies for Flexible Perovskite and Organic Photovoltaics. *Adv. Energy Mater.* **2021**, *11*, No. 2101383.
- (18) Cattaneo, G.; Faes, A.; Li, H.-Y.; Galliano, F.; Gragert, M.; Yao, Y.; Grischke, R.; Söderström, T.; Despeisse, M.; Ballif, C.; Perret-Aebi, L.-E. Lamination Process and Encapsulation Materials for Glass–Glass PV Module Design. *Photovoltaics Int.* **2015**, 82.
- (19) Ramasamy, E.; Karthikeyan, V.; Rameshkumar, K.; Veerappan, G. Glass-to-Glass Encapsulation with Ultraviolet Light Curable Epoxy Edge Sealing for Stable Perovskite Solar Cells. *Mater. Lett.* **2019**, *250*, 51–54.
- (20) Guarnera, S.; Abate, A.; Zhang, W.; Foster, J. M.; Richardson, G.; Petrozza, A.; Snaith, H. J. Improving the Long-Term Stability of Perovskite Solar Cells with a Porous Al₂O₃ Buffer Layer. *J. Phys. Chem. Lett.* **2015**, *6*, 432–437.
- (21) Matteocci, F.; Cinà, L.; Lamanna, E.; Cacovich, S.; Divitini, G.; Midgley, P. A.; Ducati, C.; Di Carlo, A. Encapsulation for Long-Term Stability Enhancement of Perovskite Solar Cells. *Nano Energy* **2016**, *30*, 162–172.
- (22) Han, Y.; Meyer, S.; Dkhissi, Y.; Weber, K.; Pringle, J. M.; Bach, U.; Spiccia, L.; Cheng, Y.-B. Degradation Observations of Encapsulated Planar CH₃NH₃PbI₃ Perovskite Solar Cells at High Temperatures and Humidity. *J. Mater. Chem. A* **2015**, *3*, 8139–8147.
- (23) Dong, Q.; Liu, F.; Wong, M. K.; Tam, H. W.; Djurišić, A. B.; Ng, A.; Surya, C.; Chan, W. K.; Ng, A. M. C. Encapsulation of Perovskite Solar Cells for High Humidity Conditions. *ChemSusChem* **2016**, *9*, 2597–2603.
- (24) Kempe, M. D.; Dameron, A. A.; Moricone, T. J.; Reese, M. O. In *Evaluation and Modeling of Edge-Seal Materials for Photovoltaic*

Applications, Conference Record of the IEEE Photovoltaic Specialists Conference, 2010; pp 256–261.

(25) Li, J.; Xia, R.; Qi, W.; Zhou, X.; Cheng, J.; Chen, Y.; et al. Encapsulation of Perovskite Solar Cells for Enhanced Stability: Structures, Materials and Characterization. *J. Power Sources* **2021**, *485*, No. 229313.

(26) Chi, W.; Banerjee, S. K. Achieving Resistance against Moisture and Oxygen for Perovskite Solar Cells with High Efficiency and Stability. *Chem. Mater.* **2021**, *33*, 4269–4303.

(27) Aranda, C. A.; Calìo, L.; Salado, M. Toward Commercialization of Stable Devices: An Overview on Encapsulation of Hybrid Organic-Inorganic Perovskite Solar Cells. *Crystals* **2021**, *11*, No. 519.

(28) Emami, S.; Martins, J.; Madureira, R.; Hernandez, D.; Bernardo, G.; Mendes, J.; Mendes, A. Development of Hermetic Glass Frit Encapsulation for Perovskite Solar Cells. *J. Phys. D: Appl. Phys.* **2018**, *52*, No. 074005.

(29) International Technology Roadmap for Photovoltaics (ITRPV); VDMA, April, 2021.

(30) Shi, L.; Young, T. L.; Kim, J.; Sheng, Y.; Wang, L.; Chen, Y.; Feng, Z.; Keevers, M. J.; Hao, X.; Verlinden, P. J.; Green, M. A.; Ho-Baillie, A. W. Y. Accelerated Lifetime Testing of Organic-Inorganic Perovskite Solar Cells Encapsulated by Polyisobutylene. *ACS Appl. Mater. Interfaces* **2017**, *9*, 25073–25081.

(31) Cheacharoen, R.; Bush, K. A.; Rolston, N.; Harwood, D.; Dauskardt, R. H.; McGehee, M. D. In *Damp Heat, Temperature Cycling and UV Stress Testing of Encapsulated Perovskite Photovoltaic Cells*, 2018 IEEE 7th World Conference on Photovoltaic Energy Conversion, WCPEC 2018—A Joint Conference of 45th IEEE PVSEC, 28th PVSEC and 34th EU PVSEC, 2018; pp 3498–3502.

(32) Fu, Z.; Xu, M.; Sheng, Y.; Yan, Z.; Meng, J.; Tong, C.; Li, D.; Wan, Z.; Ming, Y.; Mei, A.; Hu, Y.; Rong, Y.; Han, H. Encapsulation of Printable Mesoscopic Perovskite Solar Cells Enables High Temperature and Long-Term Outdoor Stability. *Adv. Funct. Mater.* **2019**, *29*, No. 1809129.

(33) Ahmad, J.; Bazaka, K.; Anderson, L. J.; White, R. D.; Jacob, M. V. Materials and Methods for Encapsulation of OPV: A Review. *Renewable Sustainable Energy Rev.* **2013**, *27*, 104–117.

(34) Cheacharoen, R.; Rolston, N.; Harwood, D.; Bush, K. A.; Dauskardt, R. H.; McGehee, M. D. Design and Understanding of Encapsulated Perovskite Solar Cells to Withstand Temperature Cycling. *Energy Environ. Sci.* **2018**, *11*, 144–150.

(35) Cheacharoen, R.; Boyd, C. C.; Burkhard, G. F.; Leijtens, T.; Raiford, J. A.; Bush, K. A.; Bent, S. F.; McGehee, M. D. Encapsulating Perovskite Solar Cells to Withstand Damp Heat and Thermal Cycling. *Sustainable Energy Fuels* **2018**, *2*, 2398–2406.

(36) Rong, Y.; Hu, Y.; Mei, A.; Tan, H.; Saidaminov, M.; Seok, S. I.; McGehee, M.; Sargent, E.; Han, H. Challenges for Commercializing Perovskite Solar Cells. *Science* **2018**, *361*, No. eaat8235.

(37) Webstore, I. IEC 61215-1:2016 *Terrestrial Photovoltaic (PV) Modules—Design Qualification and Type Approval—Part 1: Test Requirements*; International Electrotechnical Commission, 2016.

(38) Webstore, I. IEC 61215-2:2016 *Terrestrial Photovoltaic (PV) Modules—Design Qualification and Type Approval—Part 2: Test Procedures*; International Electrotechnical Commission, 2016.

(39) Bush, K. A.; Palmstrom, A. F.; Yu, Z. J.; Boccard, M.; Cheacharoen, R.; Mailoa, J. P.; McMeekin, D. P.; Hoye, R. L. Z.; Bailie, C. D.; Leijtens, T.; Peters, I. M.; Minichetti, M. C.; Rolston, N.; Prasanna, R.; Sofia, S.; Harwood, D.; Ma, W.; Moghadam, F.; Snaith, H. J.; Buonassisi, T.; Holman, Z. C.; Bent, S. F.; McGehee, M. D. 23.6%-Efficient Monolithic Perovskite/Silicon Tandem Solar Cells With Improved Stability. *Nat. Energy* **2017**, *2*, No. 17009.

(40) Shi, L.; Bucknall, M. P.; Young, T. L.; Zhang, M.; Hu, L.; Bing, J.; Lee, D. S.; Kim, J.; Wu, T.; Takamura, N.; McKenzie, D. R.; Huang, S.; Green, M. A.; Ho-Baillie, A. W. Y. Gas Chromatography–Mass Spectrometry Analyses of Encapsulated Stable Perovskite Solar Cells. *Science* **2020**, *368*, No. eaba2412.

(41) Zhang, S.; Liu, Z.; Zhang, W.; Jiang, Z.; Chen, W.; Chen, R.; Huang, Y.; Yang, Z.; Zhang, Y.; Han, L.; Chen, W. Barrier Designs in

Perovskite Solar Cells for Long-Term Stability. *Adv. Energy Mater.* **2020**, *10*, No. 2001610.

(42) Kempe, M. In *Overview of Scientific Issues Involved in Selection of Polymers for PV Applications*, Conference Record of the IEEE Photovoltaic Specialists Conference, 2011.

(43) Khenkin, M. V.; Katz, E. A.; Abate, A.; Bardizza, G.; Berry, J. J.; Brabec, C.; Brunetti, F.; Bulović, V.; Burlingame, Q.; Di Carlo, A.; Cheacharoen, R.; Cheng, Y.-B.; Colmann, A.; Cros, S.; Domanski, K.; Dusza, M.; Fell, C. J.; Forrest, S. R.; Galagan, Y.; Di Girolamo, D.; Grätzel, M.; Hagfeldt, A.; von Hauff, E.; Hoppe, H.; Kettle, J.; Köbler, H.; Leite, M. S.; Liu, S.; Loo, Y.-L.; Luther, J. M.; Ma, C.-Q.; Madsen, M.; Manceau, M.; Matheron, M.; McGehee, M.; Meitzner, R.; Nazeeruddin, M. K.; Nogueira, A. F.; Odabaşı, Ç.; Osherov, A.; Park, N.-G.; Reese, M. O.; De Rossi, F.; Saliba, M.; Schubert, U. S.; Snaith, H. J.; Stranks, S. D.; Tress, W.; Troshin, P. A.; Turkovic, V.; Veenstra, S.; Visoly-Fisher, I.; Walsh, A.; Watson, T.; Xie, H.; Yıldırım, R.; Zakeeruddin, S. M.; Zhu, K.; Lira-Cantu, M. Consensus Statement for Stability Assessment and Reporting for Perovskite Photovoltaics based on ISOS Procedures. *Nat. Energy* **2020**, *5*, 35–49.

(44) Reese, M. O.; Gevorgyan, S. A.; Jørgensen, M.; Bundgaard, E.; Kurtz, S. R.; Ginley, D. S.; Olson, D. C.; Lloyd, M. T.; Morvillo, P.; Katz, E. A.; Elschner, A.; Haillant, O.; Currier, T. R.; Shrotriya, V.; Hermenau, M.; Riede, M.; R Kirov, K.; Trimmel, G.; Rath, T.; Inganäs, O.; Zhang, F.; Andersson, M.; Tvingstedt, K.; Lira-Cantu, M.; Laird, D.; McGuinness, C.; Gowrisanker, S.; Pannone, M.; Xiao, M.; Hauch, J.; Steim, R.; DeLongchamp, D. M.; Rösch, V.; Hoppe, H.; Espinosa, N.; Urbina, A.; Yaman-Uzunoglu, G.; Bonekamp, J.-B.; van Breemen, A. J. J. M.; Girotto, C.; Voroshazi, E.; Krebs, F. C. Consensus Stability Testing Protocols for Organic Photovoltaic Materials and Devices. *Sol. Energy Mater. Sol. Cells* **2011**, *95*, 1253–1267.

(45) Mamun, A. A.; Mohammed, Y.; Ava, T. T.; Namkoong, G.; Elmustafa, A. A. Influence of Air Degradation on Morphology, Crystal Size and Mechanical Hardness of Perovskite Film. *Mater. Lett.* **2018**, *229*, 167–170.

(46) Fei, C.; Wang, H. Age-Induced Recrystallization in Perovskite Solar Cells. *Org. Electron.* **2019**, *68*, 143–150.

(47) Roose, B.; Ummadisingu, A.; Correa-Baena, J.-P.; Saliba, M.; Hagfeldt, A.; Graetzel, M.; Steiner, U.; Abate, A. Spontaneous Crystal Coalescence Enables Highly Efficient Perovskite Solar Cells. *Nano Energy* **2017**, *39*, 24–29.

(48) Bi, C.; Zheng, X.; Chen, B.; Wei, H.; Huang, J. Spontaneous Passivation of Hybrid Perovskite by Sodium Ions from Glass Substrates—Mysterious Enhancement of Device Efficiency Revealed. *ACS Energy Lett.* **2017**, *2*, 1400–1406.

(49) Meng, Q.; Chen, Y.; Xiao, Y. Y.; Sun, J.; Zhang, X.; Han, C. B.; Gao, H.; Zhang, Y.; Yan, H. Effect of Temperature on the Performance of Perovskite Solar Cells. *J. Mater. Sci.: Mater. Electron.* **2021**, *32*, 12784–12792.

(50) Schubert, M. C.; Mundt, L. E.; Walter, D.; Fell, A.; Glunz, S. W. Spatially Resolved Performance Analysis for Perovskite Solar Cells. *Adv. Energy Mater.* **2020**, *10*, No. 1904001.

(51) Domanski, K.; Roose, B.; Matsui, T.; Saliba, M.; Turren-Cruz, S.-H.; Correa-Baena, J.-P.; Carmona, C. R.; Richardson, G.; Foster, J. M.; De Angelis, F.; Ball, J. M.; Petrozza, A.; Mine, N.; Nazeeruddin, M. K.; Tress, W.; Grätzel, M.; Steiner, U.; Hagfeldt, A.; Abate, A. Migration of Cations Induces Reversible Performance Losses over Day/Night Cycling in Perovskite Solar Cells. *Energy Environ. Sci.* **2017**, *10*, 604–613.

(52) Dagar, J.; Fenske, M.; Al-Ashouri, A.; Schultz, C.; Li, B.; Köbler, H.; Munir, R.; Parmasivam, G.; Li, J.; Levine, I.; Merdasa, A.; Kegelmann, L.; Näsström, H.; Marquez, J. A.; Unold, T.; Többsens, D. M.; Schlattmann, R.; Stegemann, B.; Abate, A.; Albrecht, S.; Unger, E. Compositional and Interfacial Engineering Yield High-Performance and Stable p-i-n Perovskite Solar Cells and Mini-Modules. *ACS Appl. Mater. Interfaces* **2021**, *13*, 13022–13033.